Simultaneous spectral illumination of microplates for high-throughput optogenetics and photobiology

Arend Vogt, Raik Paulat, Daniel Parthier, Verena Just, Michal Szczepek, Patrick Scheerer, Qianzhao Xu, Andreas Möglich, Dietmar Schmitz, Benjamin R. Rost and Nikolaus Wenger

Supplementary material

Supplementary Figure 1

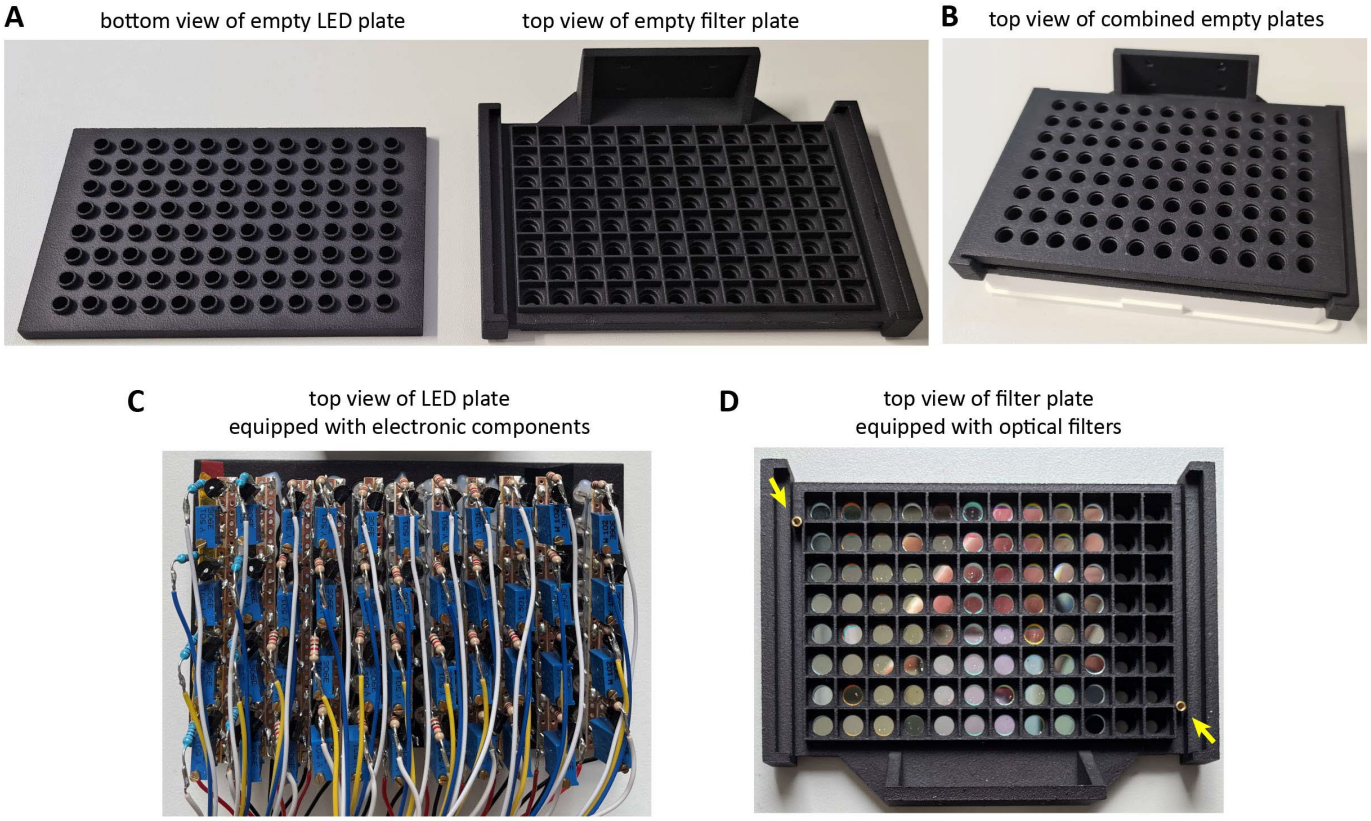

Supplementary Figure 1: Design of the illumination plate. (A) Two black subplates were 3D printed. (B) The empty subplates plugged into each other. (C) The upper plate holds the LEDs and the electronic components, consisting of the adjustable resistors, fixed resistors, and transistors. (D) The bottom plate contains the optical filters. Two columns remain without optical filters for dark control and white light LEDs. Both plates are connected with two small screws for stability (indicated with yellow arrows).

Supplementary Figure 2

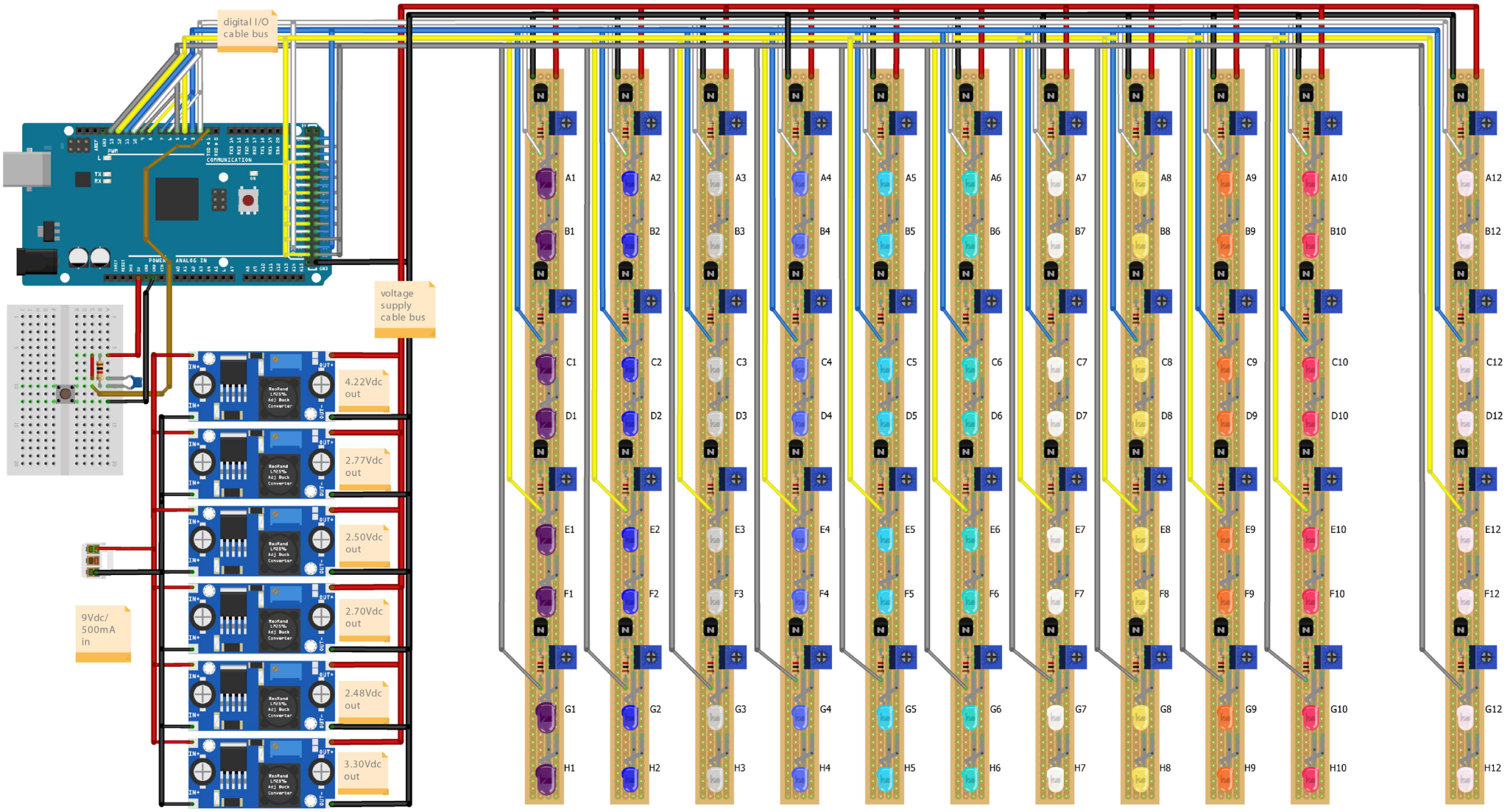

Supplementary Figure 2: Breadboard diagram of the illumination setup. Two LEDs of the same color are connected to each other and operated via a transistor, a potentiometer, and a fixed resistor. The transistor is used to control the LED on/off- state with the microcontroller digital output, while the potentiometer is used to fine-tune the light intensities. DC-DC step-down converters provide the power supply for the LEDs.

Supplementary Figure 3

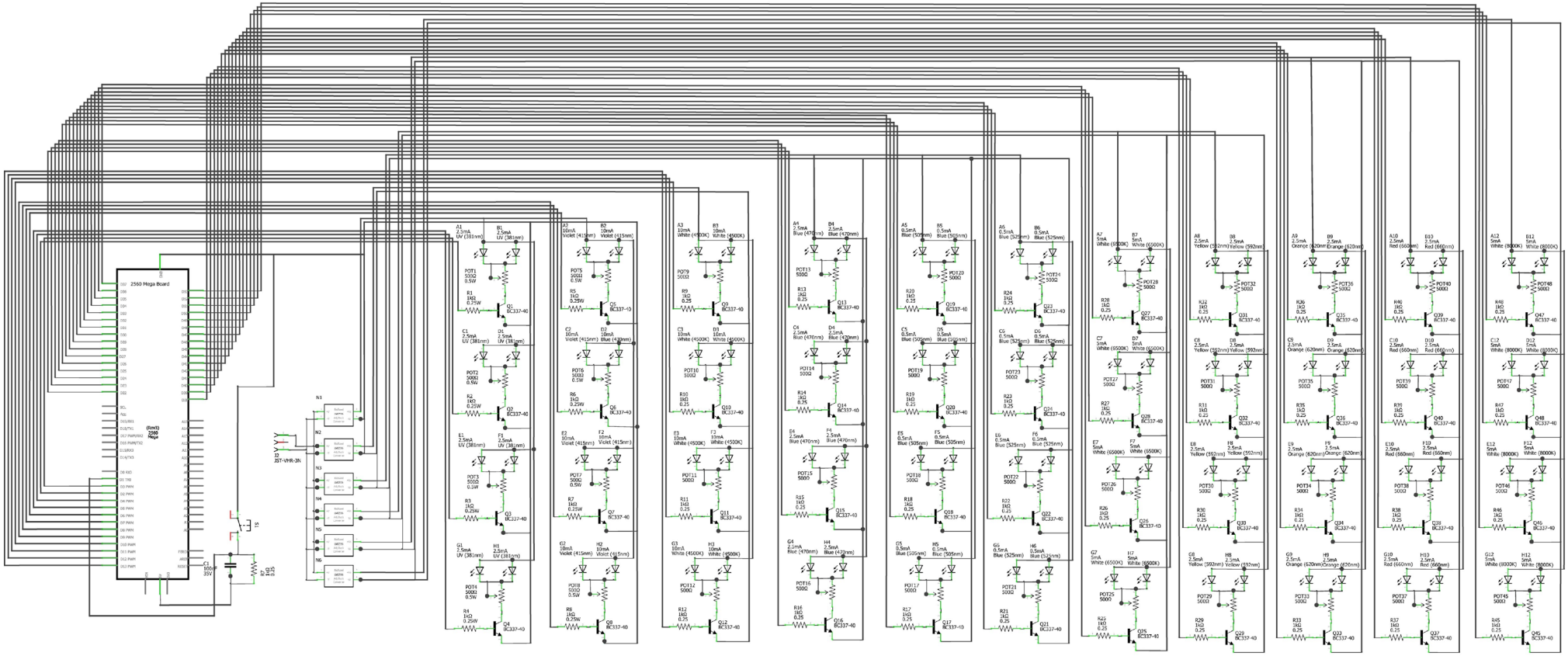

Supplementary Figure 3: Schematic circuit diagram of the illumination setup. The LEDs are controlled pairwise. Variable 500 Ω resistors in row are used to set up the forward currents of all 44 diode pairs for adjusting the desired spectral irradiance. See Methods for further details.

Supplementary Figure 4

List of LEDs and optical filters used for the RainbowCap

row	optical bandpass filter (Shenzhen Nano Macro Photonics Technology)			LEDs		max nm LED+filter
	article No.	center wavelength (CWL)	full-width at half-maximum (FWHM)	Article No. (distributor or manufacturer)	center wavelengths (CWL) in nm	
1	10312090	381 ± 2 nm	4 ± 2 nm	LL5_310 VI (Reichelt/Luckylight)	394	381
2	10310831	415 ± 5 nm	24 ± 5nm	EVL 383UBC_H2 (Reichelt/Everlight)	428	415
3	10312091	444 ± 3 nm	12 ± 3 nm	LED EL 5-22500KW (Reichelt/Everlight)	452 + 560	445
4	10310832	470 ± 3 nm	20 ± 4 nm	RND 135_00178 (Distrelec/RND Components)	468	471
5	10312092	500-505 nm	9 ± 3 nm	RND 135_00176 (Distrelec/RND Components)	503	503
6	10310833	520 ± 4 nm	20 ± 4 nm	RND 135_00038/00177 (Distrelec and Reichelt/RND Components)	520	523
7	10312093	555 ± 3nm	17 ± 3 nm	LED EL 5-23000WW (Reichelt/Luckylight)	453 + 580	556
8	10311851	592 ± 3nm	10-15 nm	RND 135_00169 (Distrelec/RND Components)	593	591
9	10310835	621-633 nm	20 ± 4 nm	LED 5-11000RT (Reichelt/Kingbright)	620	630
10	10312095	670 ± 3 nm	20 ± 3 nm	KBT L-7113HD (Reichelt/Kingbright)	660	661
11	/	/	/	/	/	dark
12	/	/	/	LED EL 5-14250WW (Reichelt/Everlight)	455 + 602	white

Supplementary Figure 5

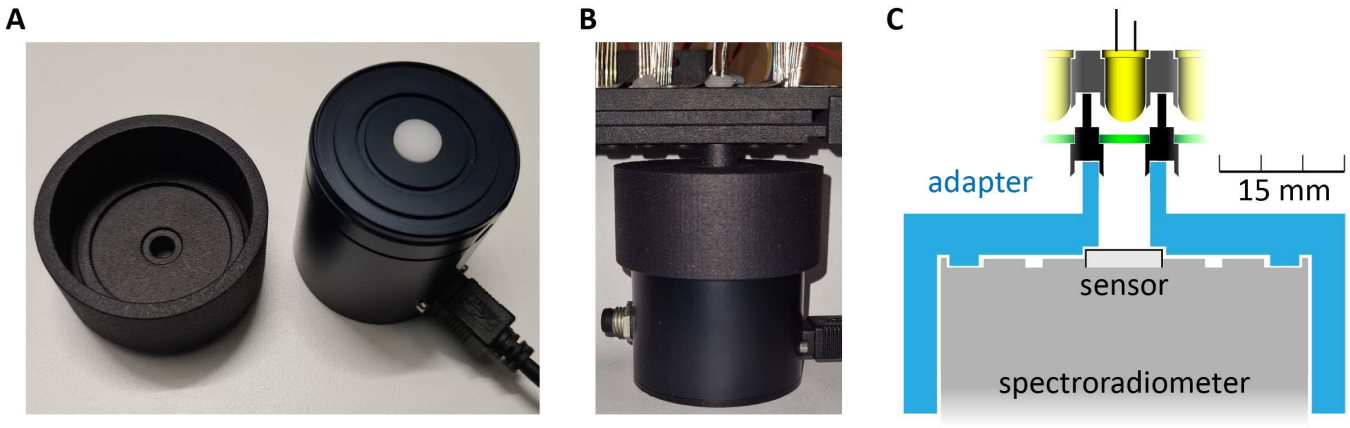

Supplementary Figure 5: Setup for measuring light intensities and emission spectra of LEDs and the LED-filter pairs. (A) Adapter specially designed for connecting LEDs (Ø 5 mm) to the spectroradiometer. (B) Photo shows the connection of an LED of the illumination plate to the adapter and the spectroradiometer. (C) Cross-section from Figure B with scale. The geometry corresponds to the architecture of the microplate illumination. Of note, the LED plate can also be plugged directly to the adapter without the optical filters.

Supplementary Figure 6

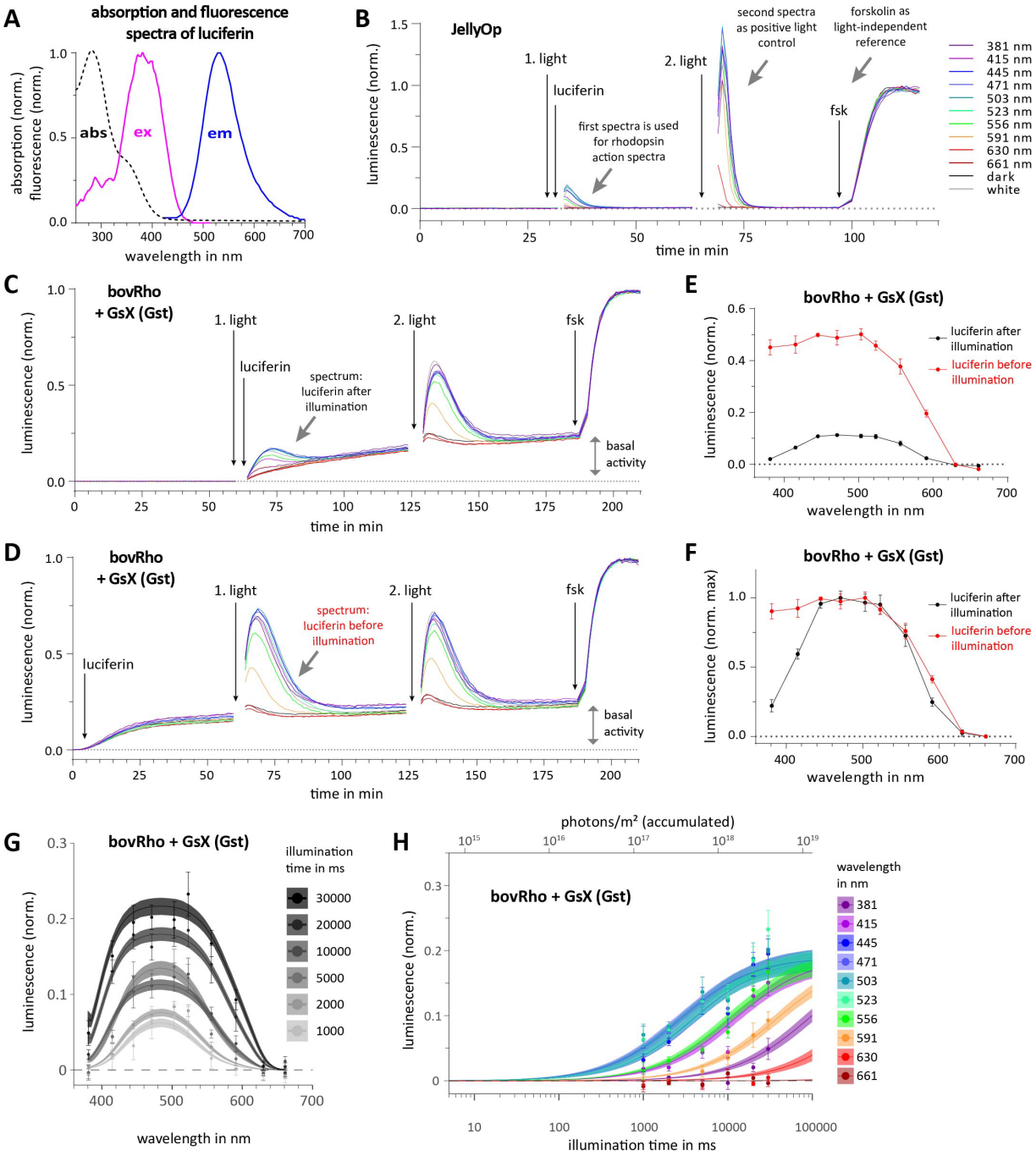

Supplementary Figure 6: Measurement of rhodopsin action spectra. (A) Absorbance, excitation, and emission spectra of luciferin measured in cell culture medium. (B) GloSensor assay with JellyOp-expressing cells and 10 s illumination time. Each curve is averaged from 4 wells. The data from the first illumination was used for determining the action spectrum. (C-D) Exemplary luminescence measurements illustrating the different luciferin application strategies. (E) Luminescence output of bovRho- and Gst-expressing cells following illumination in absence (black) or presence (red) of luciferin. Luminescence normalized to the fsk response, data points are connected without curve fit (mean ± SEM, n=4). (F) Same data as in E but normalized to the peak activity. Fluorescence of luciferin distorts the action spectra of bovRho. (G) Light titration of bovine rhodopsin. Data were fitted with the Bayesian modeling approach. The shading of the fits shows the 95 % highest density interval for estimating the divergence. Error bars represent mean ± SEM. Number of replicates is listed in Supplementary Figure 10. (H) Same data as in G but as dose-response diagram and with all tested illumination times.

Supplementary Figure 7

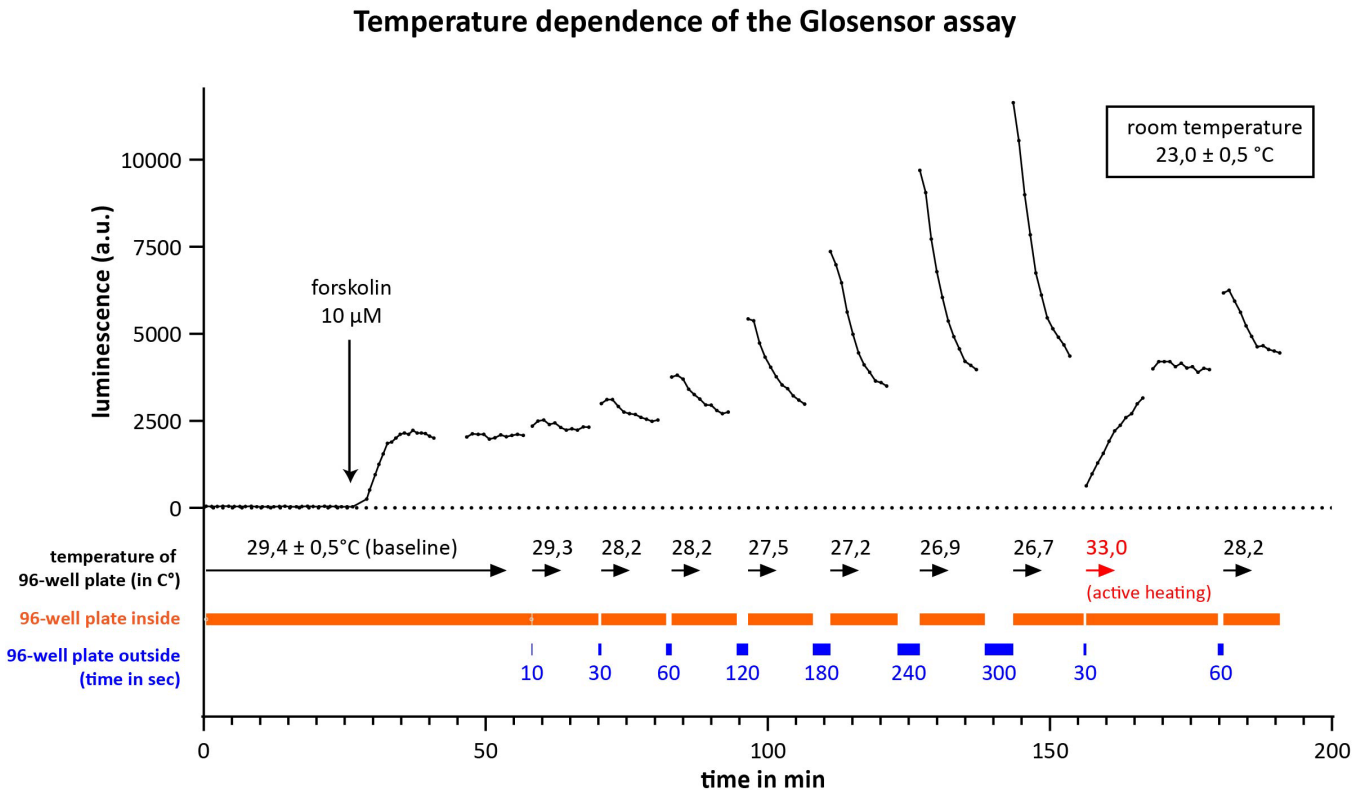

Supplementary Figure 7: The GloSensor assay is sensitive to temperature changes. We investigated the temperature effect in HEK cells transfected only with the GloSensor 22F for cAMP and stimulated the cells with forskolin (light-independent experiment). Outside the reader, the microplate cooled down due to the ambient room temperature. Note the signal increases after the microplate was put back into the reader. The luminescence signal increases proportionally with decreasing temperatures. For testing the effect of higher temperatures, the plate was placed on a heating pad for 5 s. The temperature of the microplate was measured with an infrared thermometer gun.

Supplementary Figure 8

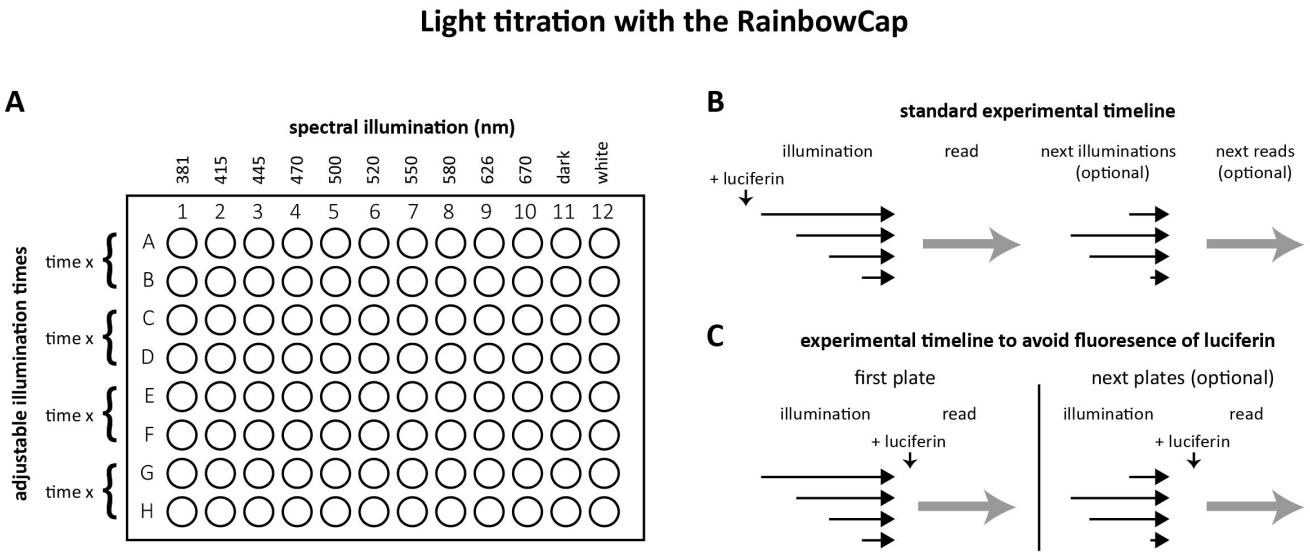

Supplementary Figure 8: The RainbowCap provides up to four illumination times for light titration. (A) The illumination time for each two rows can be controlled with the microprocessor, thus up to four different illumination times can be tested in one experiment. (B) Additional illumination times could be tested simply by repeating the experiment with other illumination times. (C) If luciferin is added after illumination, as in our Glosensor experiments with rhodopsins, other microplates must be used for additional illumination times.

Supplementary Figure 9

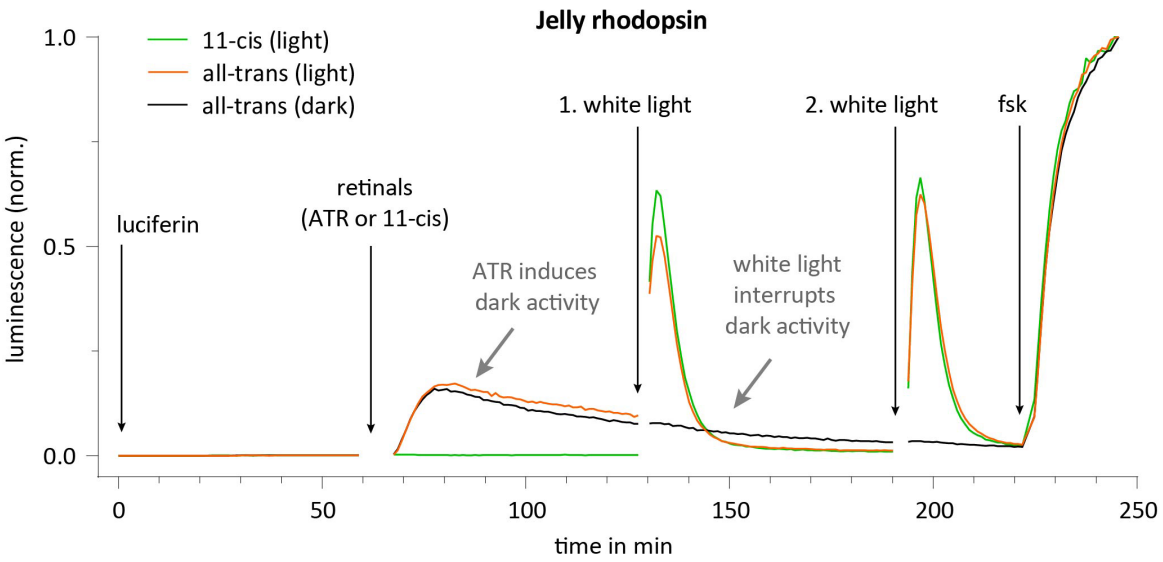

Supplementary Figure 9: Investigation of the influence of purified retinal isomers on the activity of JellyOp. HEK293TN cells were adapted to serum-free culture conditions. In the presence of luciferin, acute addition of all-trans retinal (ATR) induces dark activity in JellyOp-expressing cells. The activity slowly decays over 3 h at 29 °C (black trace). Dark activity is not seen after addition of 11-cis retinal (green trace). Illumination with white light for 10 s stops the ATR-induced dark activity. Each trace corresponds to data from one well.

Supplementary Figure 10

Overview of replicates used for the diagrams

experiment	replicates			used for figures
	Illumination times in ms	number of pooled wells from several plates	number of independent experiments (=number of plates)	
Light titration of JellyOp	60000 50000 30000 20000 10000 5000 2000 1000 500 200 100 50 10	5 5 4 6 15 8 8 7 6 6 2 7 4	3 3 3 4 6 4 5 4 3 4 1 4 2	3D 3E 3F 3G
Light titration of bovRho	30000 20000 10000 5000 2000 1000	8 7 15 8 5 7	4 4 5 4 3 4	3D 3G S-6G S-6H
Light titration of bPAC-wt	60000 50000 40000 30000 25000 20000 15000 10000 5000 2000 1000 500 50	4 5 4 4 3 3 8 9 12 4 3 5 8	4 4 3 4 3 3 5 5 7 4 3 4 6	4B 4C S-11C S-11F
Light titration of bPAC-S27A	60000 50000 40000 30000 25000 20000 15000 10000 5000 2000 1000 500 50	4 3 4 4 3 3 8 11 8 4 3 5 4	4 3 4 4 3 3 5 6 5 4 3 4 4	4B 4C S-11D S-11G
Light titration of DmPGC	60000 50000 40000 30000 20000 15000 10000 5000 2000 1000 500 50	6 8 6 6 8 10 16 8 6 6 6 6	3 4 3 3 4 5 4 4 3 3 3 3	4B S-11E S-11H
reconstitution of JellyOp with retinal isomers	10000 (13-cis retinal) 10000 (11-cis retinal) 10000 (9-cis retinal)	12 11 13	7 5 5	3H 3I

Supplementary Figure 11

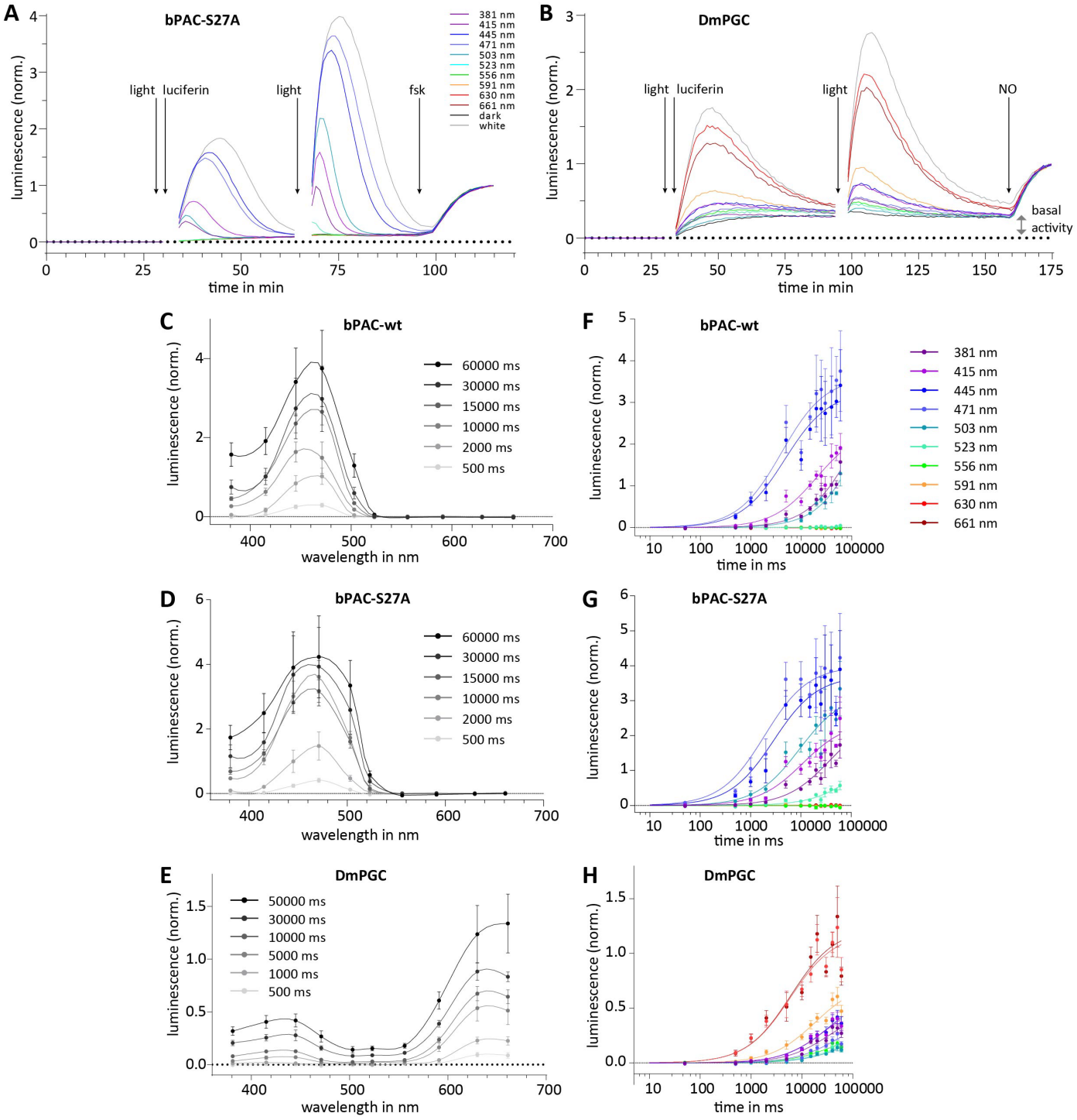

Supplementary Figure 11: Investigation of photoactivated cyclases. (A-B) GloSensor measurements of cells expressing bPAC-S27A (15 s illumination) or DmPGC (10 s illumination). All data were normalized to peak signals achieved with pharmacological induction of cAMP (10 µM forskolin [fsk] for stimulation of adenylyl cyclases), or cGMP (25 µM nitric oxide [NO] for stimulation of guanylyl cyclases). Each curve represents the mean value of 4 individual wells of the same plate. The cGMP-GloSensor shows basal activity independent of optogenetic proteins. (C-E) Action spectra and light titration of cyclases. Curves were fitted with spline fits. (F-H) Log scale plots of the data from C-E. Curves were fitted with dose-response equation. Data points in C-H are indicated as mean ± SEM (n-values in Suppl. Figure 10).

Supplementary Figure 12

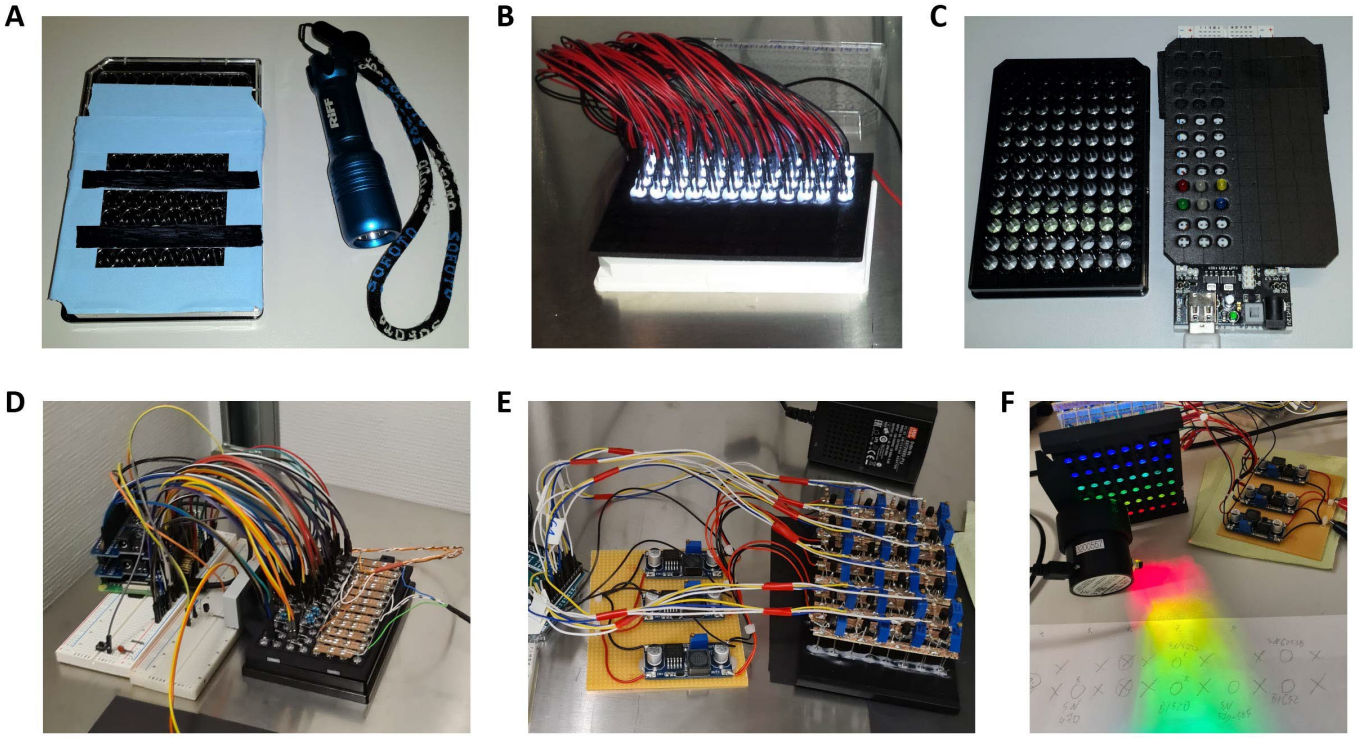

Supplementary Figure 12: Evolution of the RainbowCap illumination device. (A) Illumination of microplates with simple flashlights. (B) 48 white LEDs mounted on a board for microplates. The wells without light can be used as dark controls. (C) Implementing a microcontroller for advanced control of light sources. (D) First prototype for simultaneous spectral illumination. Luminescence-based assays need illumination from top. (E) First prototype with the power management finally used, but with only 6 LED columns. (F) First prototype with the combination of LEDs and optical filters but with only 6 different colors.

Supplementary Figure 13

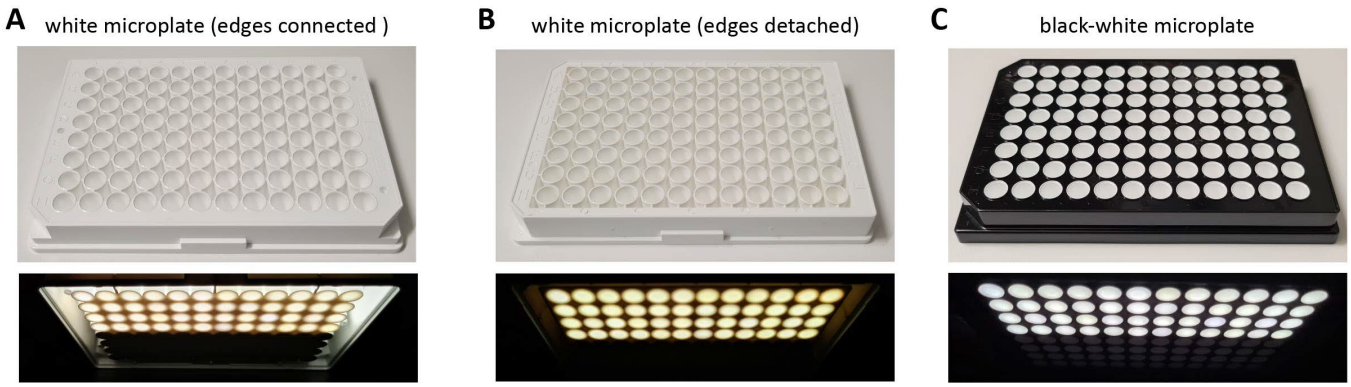

Supplementary Figure 13: The structure and color of microplates influence the spillover of light into neighboring wells. 4 of 8 rows were illuminated with white light. (A) Standard white plate for luminescence with connected edges. Note that the light spreads around the wells. (B) Standard white plate for luminescence with detached edges ("chimney design"). The different plate architecture reduces light spread. (C) Black plate with white wells for best light protection between the wells.

Supplementary Methods

Fitting the action spectra of rhodopsins to a Govardovskii nomogram by using Bayesian hierarchical modeling

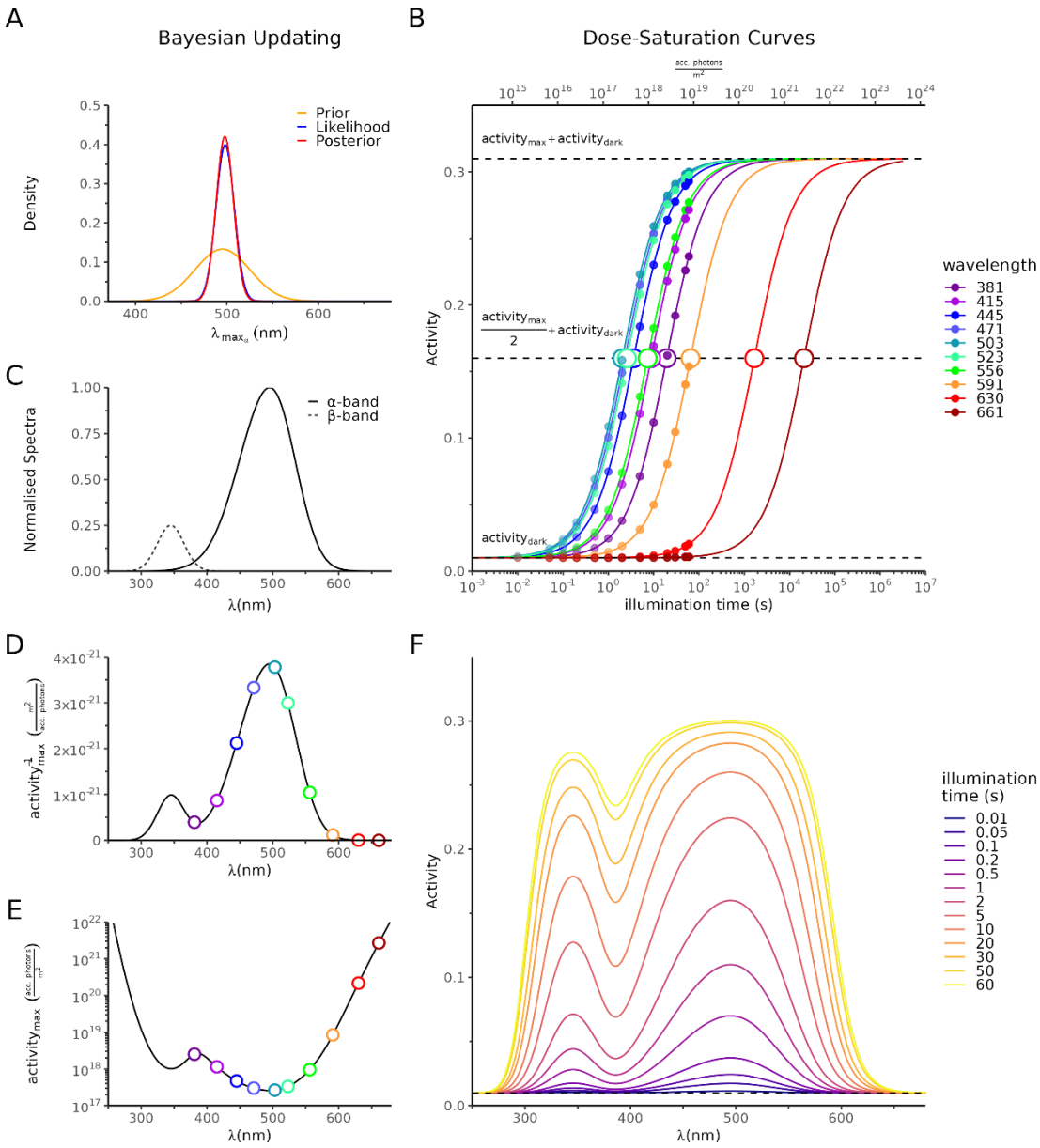

Figure 1: A: Schematic of an exemplary parameter λ_{max_α} with a prior distribution (yellow), the likelihood of the data (blue) and the resulting posterior distribution (red) by applying the Bayes theorem. B: Different illumination times (corresponding to different photon counts) plotted against the Glosensor activity for each wavelength (filled dots). These measurements

can be used to estimate I_{50_λ} (circles) and $activity_{max}$. Additional dark activity information is used in the model to allow for appropriate scaling. C: The Govardovskii template is applied to estimate the α- and β-bands, which are summed up to obtain a normalized spectrum that can be used to fit the I_{50_λ} (D and E). The estimated I_{50_λ} and $activity_{max}$ from the dose-saturation curve then describe the collected data and the underlying activity spectra. The estimated parameters are then applied in the dose-saturation equation to fit the activity spectra with varying photon exposure (F).

Govardovskii template

The rhodopsin nomogram developed by Govardovskii et al. (Govardovskii et al. 2000) was used as a basis for describing the α-band and β-band of the spectrum:

$$S_\alpha(x) = \frac{1}{e^{A(a-x)} + e^{B(b-x)} + e^{C(c-x)} + D}$$

$$S_\beta(\lambda) = Ae^{-\left((\lambda-\lambda_{m\beta})/b\right)^2}$$

Bayesian framework:

In a Bayesian framework we estimate the spectral density not as a single estimate but a distribution of probable outcomes (posterior distribution: $P(M \mid y)$), which are in line with the already existing information about parameters (prior distribution: $P(M)$) weighted by the likelihood ($P(y \mid M)$) of the experimental data (y).

$$P(M \mid y) \propto P(M)P(y \mid M)$$

Starting points for parameters were informed using Govardovskii et al. (Govardovskii et al. 2000) as basis for model parameter priors with added uncertainty. For the construction of the model, we followed the workflow proposed by Gabry et al. (Gabry et al. 2019) simulating data first, testing the model and then applying the model to the real data set. First, we tested whether the parameter values proposed by Govardovskii et al. (Govardovskii et al. 2000) are appropriate to fit to our data. For this we compared the fixed parameters model, which excludes the possibility of adjusting for shape differences, as proposed by Govardovskii et al. (Govardovskii et al. 2000), with a flexible parameter version of the model. The fixed-parameter model performed worse when comparing the model's expected log pointwise predictive density (ELPD) as described by Vehtari et al. (Vehtari et al. 2017). This suggests that the self-adjusting parameter model describes the observed activity better than the fixed parameter model. Hence fitting the activity spectra was performed using the model with non-fix parameters.

Estimation of dark activity:

Dark activity (y_{Dark}) is defined as the Glosensor activity recorded prior to any light activation of the construct. This activity has to be subtracted from the light-induced activity and can be described by a gamma distribution with a shape parameter (k_{Dark}) and the mean (μ_{Dark}). The mean of the dark activity is estimated by combining a general activity independent of the group (β_{dark}) with group specific dark activity ($\gamma_{Dark}X_{Group}$) and inter-experiment variability ($Z_{Dark_{exp}}, Z_{DarkGroup_{exp}}$).

$$\mu_{Dark_i} = e^{\beta_{Dark}+\gamma_{Dark}X_{Group_i}+Z_{Dark_{exp}}+Z_{\gamma_{Dark_{exp_i}}}X_{Group_i}}$$
$$y_{Dark_i} \sim Gamma\left(k_{Dark}, \frac{k_{Dark}}{\mu_{Dark_i}}\right)$$

Estimation of λ_{max_α} and λ_{max_β}:

The α- and β-peaks are estimated for the different construct groups ($\gamma_{\lambda_{max}}X_{Group}$) and include experimental variability between well plates in the parameters ($Z_{\lambda_{max_{\alpha exp}}}$).

$$\lambda_{\max_{\alpha i}} = e^{\lambda_{max_\alpha}+\gamma_{\lambda\max_\alpha}X_{Group_i}+Z_{\lambda\max_{\alpha exp_i}}}$$
$$\lambda_{max_{\beta_i}} = \beta_{\max 1} + \beta_{\max 2}\lambda_{max_{\alpha i}}$$

Estimation of the normalized spectrum:

The normalized spectrum (S) is calculated by adding the different normalized spectra to the α- and β-peak, respectively.

$$a_{\alpha_i} = a_{1_\alpha} + a_{2_\alpha}e^{-\frac{\left(\lambda_{max_{\alpha_i}}-300\right)^2}{11940}}$$
$$b_{\beta_i} = b_\beta + \omega_\beta\lambda_{max_{\alpha i}}$$
$$x_{i,\lambda} = \frac{\lambda_{max_{\alpha i}}}{\lambda}$$
$$S_\alpha(x_{i,\lambda}) = \frac{e^{A_\alpha\left(a_{\alpha_i}-1\right)+B_\alpha\left(b_{\alpha_i}-1\right)+C_\alpha\left(c_{\alpha_i}-1\right)+D_\alpha}}{e^{A_\alpha\left(a_{\alpha_i}-x_{i,\lambda}\right)+B_\alpha\left(b_{\alpha_i}-x_{i,\lambda}\right)+C_\alpha\left(c_{\alpha_i}-x_{i,\lambda}\right)+D_\alpha}}$$
$$S_\beta(x_{i,\lambda}) = A_\beta e^{-\left(\frac{\lambda-\lambda_{max_{\beta_i}}}{b_{\beta_i}}\right)^2}$$
$$S_{total}(x_{i,\lambda}) = \frac{S_\alpha(x_{i,\lambda}) + S_\beta(x_{i,\lambda})}{1 + S_\beta\left(\lambda_{max_{\beta_i}}\right)}$$

Scaling of normalized spectrum to fit activity spectra:

To fit activity spectra amplitudes, we utilized a hierarchical version of a dose-saturation curve, incorporating information about experimental and construct differences for different wavelengths. The mean amplitude for a given construct, experiment, illumination time, and wavelength ($\mu_{i,\lambda}$) is the sum of the dose-saturation curve and existing dark activity.

$$\mu_{i,\lambda} = \frac{activity_{max_i}[t_i]}{I_{50_{i,\lambda}} + [t_i]} + \mu_{Dark_i}$$

The illumination times (t) can be considered parts of the substrate for opsin activation as they are proportional to photon exposure. The relative sensitivity at different wavelengths (λ) represented by A_{1_λ} can be described by a scaled inverse of the Govardovskii template (Fig. 1E).

$$activity_{max_i} = activity_{max} e^{Z_{activity_{max exp_i}} + \gamma_{activity_{max}} X_{Group_i}}$$
$$I_{50_{i,\lambda}} = \frac{I_{50_{scale}} e^{\gamma_{I_{50}} X_{Group_i}}}{S_{total}(x_{i,\lambda})}$$

The data are fitted using a Gamma distribution (positive continuous) with a shape (α) and an experiment specific rate parameter (β_{exp}). The shape parameter α of the distribution can be written to include the mean (μ). Here the mean activity for any given construct, experiment, and wavelength ($\mu_{i,\lambda}$) is the sum of the dark activity for the construct and experiment (μ_{Dark_i}) and the estimated activity for the construct, experiment, illumination time, and wavelength ($v_{i,\lambda}$).

$$\beta_{exp_i} = \beta e^{Z_{\beta_{exp_i}} + Z_{\beta_{Group_i}}}$$
$$\alpha_{i,\lambda} = \frac{\beta_{exp_i}}{\mu_{i,\lambda}}$$
$${\sigma^2}_{i,\lambda} = \frac{\alpha_{i,\lambda}}{\beta_{exp_i}}$$
$$y_{i,\lambda} \sim Gamma\left(\alpha_{i,\lambda}, \beta_{exp_i}\right)$$

Peak wavelength of activity spectra:

As described by Govardovskii et al. (Govardovskii et al. 2000) reading the parameters λ_{max_α} alone might not be meaningful depending on the other parameters and does not reflect the overall maximum. However, the peak (λ_{Peak}) can be calculated by finding the wavelength (λ) which maximizes the function for the normalized spectrum:

$$\lambda_{Peak_i} = \arg\max_{\lambda} S_{total}(x_{i,\lambda})$$

This peak reflects the mixture of α- and β-components and is the location of the total maximum activity.

Parameter Priors:

Parameters for the Govardovskii template:

$$\lambda_{max_\alpha} \sim e^{Normal(\log(498),0.07)}$$
$$A_\alpha \sim Gamma(80,80/69.7)$$
$$B_\alpha \sim Gamma(20,20/28)$$
$$C_\alpha \sim Normal(-14.9,5)$$
$$D_\alpha \sim Normal(0.674,0.05)$$
$$\alpha_{1_\alpha} \sim \text{logit}^{-1}(Normal(1.9877,0.45))$$
$$\alpha_{2_\alpha} \sim Normal(0.0459,0.01)$$
$$b_\alpha \sim \text{logit}^{-1}(Normal(2.4698,0.5))$$
$$c_\alpha \sim Normal(1.104,0.1)$$

$$A_{\beta_k} \sim Gamma(5,0.05)$$
$$A_{\beta_\mu} \sim Gamma(10,10/0.26)$$
$$A_\beta \sim Gamma\left(A_{\beta_k}, A_{\beta_k}/A_{\beta_\mu}\right)$$
$$\beta_{\max 1} \sim Gamma(500,500/189)$$
$$\beta_{\max 2} \sim Gamma(300,300/0.315)$$
$$b_\beta \sim Normal(-40.5,10)$$
$$\omega_\beta \sim Gamma(20,20/0.195)$$

Estimation of dark activity:

$$k_{Dark} \sim Gamma(4,4/15)$$
$$\gamma_{Dark} \sim StudentT(3,0,1)$$
$$\beta_{Dark} \sim Normal(\log(0.025)\,,1)$$

Estimation of dose-saturation curve:

$$activity_{max} \sim Gamma(7,/0.3)$$
$$I_{50_{scale}} \sim Gamma(4,4/7500)$$

Estimation of group (opsin/retinal) specific parameters:

$$\gamma_{\lambda_{\max_\alpha}} \sim Normal(0,0.05)$$
$$\gamma_{A_1} \sim Normal(0,0.5)$$
$$\gamma_{A_0} \sim Normal(0,1)$$
$$\tau_{\beta_{Group}} \sim Normal^{+}(0,0.5)$$
$$Z_{\beta_{Group}} \sim Normal\left(0, \tau_{\beta_{Group}}\right)$$

Estimation of experimental hierarchy:

$$\tau_{\lambda_{\max_{\alpha\,exp}}} \sim Normal^{+}(0,0.0025)$$
$$\tau_{\gamma_{\lambda_{\max_{\alpha\,exp}}}} \sim Normal^{+}(0,0.05)$$
$$\tau_{Dark_{exp}} \sim Normal^{+}(0,0.5)$$
$$\tau_{\gamma_{Dark_{exp}}} \sim Normal^{+}(0,0.05)$$
$$\tau_{activity_{max_{exp}}} \sim Normal^{+}(0,0.0025)$$
$$\tau_{\beta_{exp}} \sim Normal^{+}(0,0.1)$$
$$\Omega = \Omega_L \Omega_L^T$$
$$\Sigma = (diag(\tau)\Omega_L)(diag(\tau)\Omega_L^T)^T$$
$$\Omega \sim LKJCorr(2)$$
$$Z_{exp} \sim MultivariateNormal(0, \Sigma)$$

Link to repository:

https://github.com/danielparthier/Vogt-et-al-2024

References:

Gabry, J., Simpson, D., Vehtari, A., Betancourt, M., Gelman, A. (2019). Visualization in Bayesian Workflow. Journal of the Royal Statistical Society Series A: Statistics in Society 182: 389-402.

Govardovskii, V. I., Fyhrquist, N., Reuter, T., Kuzmin, D. G., Donner, K. (2000). In search of the visual pigment template. Visual Neurosci 17: 509-528.

Vehtari, A., Gelman, A., Gabry, J. (2017). Practical Bayesian model evaluation using leave-one-out cross-validation and WAIC (vol 27, pg 1413, 2017). Stat Comput 27: 1433-1433.